

Corticofugal modulation of the information processing in the auditory thalamus of the cat

A.E.P. Villa, E.M. Rouiller*, G.M. Simm, P. Zurita, Y. de Ribaupierre, and F. de Ribaupierre

Institut de Physiologie, Université de Lausanne, Rue du Bugnon 7, CH-1005 Lausanne, Switzerland

Received October 22, 1990 / Accepted April 24, 1991

Summary. Single unit activity of 355 cells was recorded in the auditory thalamus of anesthetized cats before, during, and after the inactivation by cooling of the ipsilateral primary auditory cortex (AI). Most of the units ($n=288$) showed similar functional characteristics of firing before and after the cryogenic blockade of AI. The spontaneous firing rate remained unchanged by cooling in 20% of the units and decreased in the majority of them (60%). In some regions, i.e. dorsal division of the medial geniculate body (MGB), lateral part of the posterior group of the thalamus, and auditory sector of the reticular nucleus of the thalamus, the maximum firing rate evoked by white noise bursts was generally affected by cooling in the same direction and to the same extent as the spontaneous activity. Units in the ventral division of MGB showed a characteristic increase of signal-to-noise ratio during cortical cooling. The corticofugal modulation led to the appearance or disappearance of the best frequency of tuning in 51 units and changed it by more than 0.5 octave in 34 units. The bandwidths of different response patterns to pure tones stimulation were used to define a set of functional properties. During cryogenic blockade of AI, two cortically modulated sub-populations of units were usually distinguished that exhibited changes for a given functional property. The complexity and diversity of the effects of cortical inactivation suggest that the corticothalamic projection may be the support for selective operations such as an adaptive filtering of the incoming acoustic signal at the thalamic level adjusted as a function of cortical activity.

Key words: Cryogenic blockade – Corticofugal modulation – Spontaneous activity – Acoustically driven activity – Temporal response pattern – Adaptive filtering – Cat

Introduction

The medial geniculate body (MGB) is the main nucleus of the auditory thalamus (Rose and Galambos 1952; Morest 1964). Based on cytoarchitectonics, the MGB of the cat has been subdivided into dorsal, ventral, and medial divisions. These subdivisions roughly correspond to parallel ascending auditory pathways (Calford and Aitkin 1983; Winer 1988). The dorsal division (D) sends its projections mainly to the secondary auditory cortex (AII) (Winer et al. 1977; Andersen et al. 1980). The ventral division of the MGB is known to be tonotopically organized (Purser and Whitfield 1972; Aitkin and Webster 1972; Morel et al. 1987) and it is subdivided into pars lateralis (LV) and pars ovoidea (OV). The cortical targets of LV and OV are the tonotopically organized primary (AI), anterior, and posterior auditory fields (Andersen et al. 1980; Morel and Imig 1987). The medial division of MGB (M) projects to all the auditory cortical fields (Morel and Imig 1987; Rouiller et al. 1989). The laminar distribution of this projection is very different from that of the ventral and dorsal divisions because the relay cells of M send axons into the cortical layer I, whereas the relay cells of the other divisions send their axons to cortical layers IV and VI (Mitani et al. 1987).

All divisions of the MGB receive descending influences directly by corticofugal projections (Andersen et al. 1980) and via the reticular nucleus of the thalamus (RE) (Jones 1975; Rouiller et al. 1985; Villa 1990). The other thalamic nuclei related to the auditory pathway are the lateral part of the posterior group of the thalamus (POL) (Heath and Jones 1971; Morel and Imig 1987), the supragenulate nucleus (SG) (Winer 1988), and the nucleus of the brachium of the inferior colliculus (BIN) (Morest 1964).

Thalamocortical and corticothalamic pathways generally establish reciprocal connections (Andersen et al. 1980), although local discontinuities have been reported (Winer 1988). The role and nature of corticofugal projections have been extensively investigated but controversial data have been reported in the literature of the auditory pathway. Several authors suggested an inhibitory role of

* Present address: Institut de Physiologie, Université de Fribourg, Pérolles, CH-1700 Fribourg, Switzerland
Offprint requests to: A.E.P. Villa (address see above)

the corticofugal projections (Desmedt and Mechelse 1958; Watanabe et al. 1966; Amato et al. 1969), whereas others did not report any corticofugal effect on the thalamus (Aitkin and Dunlop 1969). Complex effects, mixing excitations, and inhibitions have been reported (Ryugo and Weinberger 1976) and a clearly excitatory or facilitatory role has also been suggested (Orman and Humphrey 1981).

Thalamo-cortical integration and cortico-thalamic feedback represent a general feature of the sensory channels in the central nervous system. Parallel pathways in the sensory systems might be described to some extent (Diamond 1983). It is of interest to notice that evidence from studies in the visual (Kalil and Chase 1970; Singer 1977; Tsumoto et al. 1978) and somatic (Macchi et al. 1986; Yuan et al. 1986) systems show that corticofugal fibers excite the principal sensory nuclei of the thalamus.

The purpose of the present study is to clarify the controversy on the nature of the corticothalamic projections in the auditory thalamus by reversibly inactivating the primary auditory cortex (AI) by means of cortical cooling while recording single unit responses in histologically identified thalamic nuclei. The spontaneous and acoustically driven activity of each unit was studied before, during, and after the cortical blockade. New forms of data presentation are introduced in order to investigate in more detail than previously the functional significance of the corticothalamic projection. The data have been acquired by simultaneous recordings from independently driven microelectrodes (Villa 1988). This study focuses on the corticofugal effects of cooling on single unit activities, preliminarily described in previous abstracts (Villa et al. 1984; Villa et al. 1989). The effects of cooling on neuronal interactions are discussed elsewhere (Villa et al., in preparation).

Methods

Surgical preparation

The surgical, stimulating, and recording procedures were basically the same as previously described (Villa 1988; Rodrigues-Dagaëff et al. 1989). Nine cats of either sex weighing 1.5–2.9 kg were used. Anesthesia was induced by sodium pentobarbital (Nembutal, 40 mg/kg/i.p.); all wounds were treated with the permanent local anesthetic Effocaine. The arterial blood pressure, heart rate, and body temperature were continuously monitored. Each cat was placed in a stereotactic instrument without earbars and was oriented with respect to Horsley-Clarke reference planes. Two holes (diameter 12 mm) were drilled through the skull, leaving the dura mater intact. One supported the microelectrodes device which was positioned stereotactically, the other the cooling chamber, which was positioned using the suprasylvian sulcus and the dorsal end of the anterior and posterior ectosylvian sulci as landmarks (Fig. 1).

After the surgery the cats were paralyzed with gallamine thiethiodide (Flaxedil, 10 mg/kg per hour) and artificially ventilated with a mixture of 80% N₂O and 20% O₂ throughout the recording sessions. The reflex state was periodically checked by twisting the limbs and observing the pupil size. In addition to the nitrous oxide, subsequent injections of Rompun (3 mg/kg/i.m.), or Nembutal (10 mg/kg/i.v.), or Ketalar (15 mg/kg/i.v.) were sometimes needed one or two times per 24 hours. The recording session was suspended

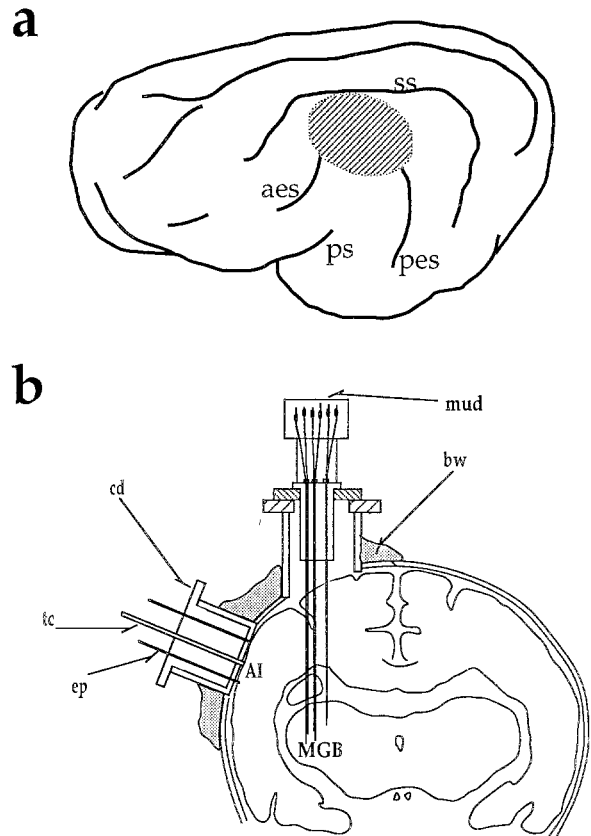


Fig. 1. **a** Brain diagram of the left hemisphere of the cat with a shaded ring representing the approximate position of the cooling probe. aes: anterior ectosylvian sulcus; pes: posterior ectosylvian sulcus; ps: pseudosylvian sulcus; ss: suprasylvian sulcus. **b** Diagram of a coronal section of the skull showing the geometric relations between the major elements of the experimental setup. AI: primary auditory cortex; MGB: medial geniculate body; bw: bone wax and dental cement; cd: cooling probe; ep: microelectrode for recording the evoked potential; mud: multiple microelectrode device for single unit recording; tc: thermistor

for a couple of hours after these injections. The effect of these drugs has been described elsewhere (Zurita et al. 1988).

A recording session, 60 hours on average, started about 16–20 h after the beginning of surgery; at the end the animals were deeply anesthetized with Nembutal. Electrolytic lesions were performed at a known depth for reconstruction of the recording sites. The histological and track reconstruction procedures have been described elsewhere (Rodrigues-Dagaëff et al. 1989).

Cooling technique

The cooling device consisted of an aluminium cylindrical core (diameter 10 mm, height 18 mm), refrigerated by circulating ice-cold water at a constant flux of 0.1 l/min, in tight contact with the dura mater. The thermic gradient beneath the cooling device and the cooling kinetics were evaluated in a model by recording the temperature from six thermocouples, separated by one mm in depth, placed in an agar block (diameter 20 mm, height 20 mm) surrounded by circulating water at 38°C. This simulation, repeated three times, showed that a steady-state was reached 20 minutes after the beginning of cooling, characterized by a temperature of 22°C, 5 mm beneath the surface (Fig. 2). Such temperature has been reported to induce an inactivation of cortical synapses (Brooks 1983).

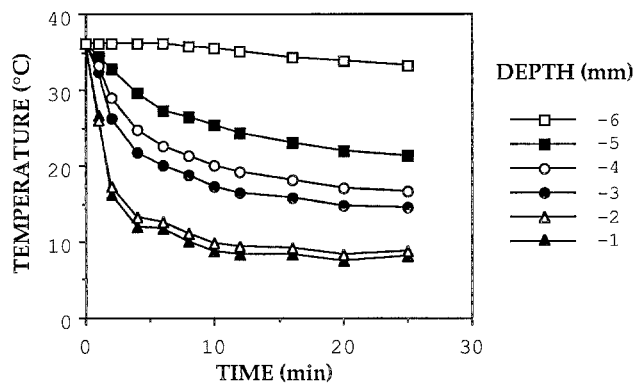


Fig. 2. Diagram of cooling kinetics and thermic gradient estimated by six thermocouples separated by 1 mm in depth, placed in an agar block beneath the cooling device and surrounded by circulating water at 38°C. Note that the gradients at 1 and 2 mm beneath the surface are very similar, probably due to the poor effect of the circulating warm fluid at these depths

Five holes were drilled in the cylinder for a thermocouple and for the microelectrodes monitoring the auditory evoked responses. The thermocouple monitored the temperature close to the surface of the cortex. The thermocouple recording and the observation of the evoked potentials showed that a steady-state was reached in 18 ± 3 min after the onset of cooling. Thus, the kinetics evaluated during cooling of the agar block was assumed to be a good estimation of the kinetics operating in the living brain. Cortical rewarming was achieved by interrupting the cooling fluid; return to the physiological state showed kinetics similar to those for cooling. Although portions of surrounding cortical fields may have been affected by a lateral spread of cooling, we will refer to AI inactivation in the Results section.

Data recording and analysis

Single unit recordings in the auditory thalamus were made with glass-coated platinum-plated tungsten microelectrodes of an impedance in the range 0.5–2 M Ω measured at a frequency of 1 kHz. The experiments were performed with a multielectrode device. Up to six microelectrodes, each driven independently by DC micromotors, were advanced through stereotaxically oriented guides. The electrode depth was evaluated by measuring changes in electric capacitances dependent on the linear advance of the electrodes, with an accuracy of 5 μ m. An analog multi-unit analyzer was used to perform on-line spike-train separation (Ivarsson et al. 1988). The epochs of detected neural events were recorded by a PDP 11/24 microcomputer and stored digitally for off-line analysis. Dot rasters (dot-displays) were displayed in real-time.

The inactivation of the primary auditory cortex was monitored by the shape of the evoked potentials recorded from 4 cut glass-coated tungsten microelectrodes (tip diameter 50–70 μ m) placed near the edge of the cooling probe, and sampling different places of the auditory cortex beneath the cooling probe. The electric signal was amplified and passed through an analog/digital converter before sending it to the microcomputer for averaging (Fig. 3). Two macroelectrodes were fastened to the unopened skull of the cat to record a bipolar electroencephalogram (EEG). One electrode was placed in the frontal bone and the other in the occipital bone. The EEG was periodically used to check if changes occurred in the arousal state of the cat.

Data analysis was performed by the computation of histograms of time series in single unit spike trains. The peristimulus time histograms (PST) and autocorrelograms, namely autorenewal density histograms (ARD), were calculated off-line according to Abeles

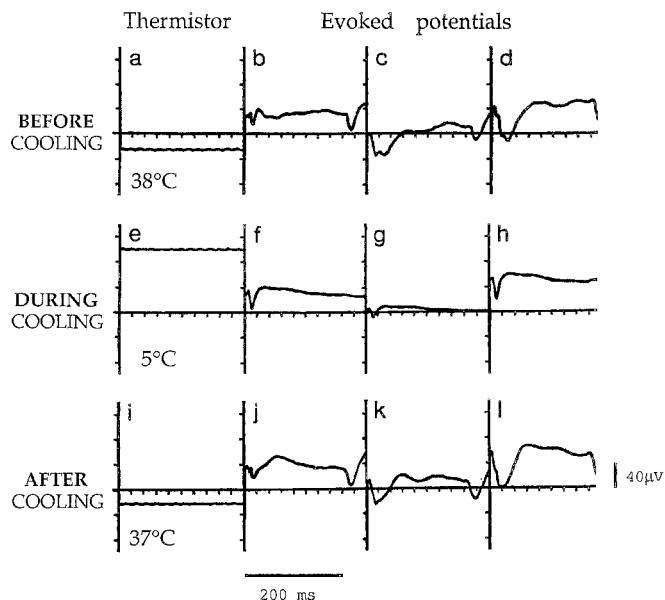


Fig. 3a–l. Thermistor recording and auditory evoked potentials from the primary auditory cortex before (a–d), during (e–h) and after (i–l) the cooling of that area. The recordings labeled (b, f, j), (c, g, k) and (d, h, l) correspond to an average of 100 potentials recorded from three electrodes. The horizontal scale for all recordings is 25 ms per subdivision and the duration of the auditory stimulus (200 ms) is indicated by a horizontal bar. The vertical scale for the thermistor recording is 10°C and for the evoked potentials 40 μ V per subdivision. Note during cooling the weak transient onset evoked response due to the ascending thalamic input. This response indicates that the electrical activity is preserved in the thalamo-cortical fibers

(Abeles 1982a). Using this technique all histograms were scaled in rate units (spikes/s) and they were smoothed by a convolution with a moving Gaussian shaped bin. For each histogram, the 99% confidence limits were calculated, assuming that a Poisson distribution underlaid the spike train discharges.

Any significant deviations from a random Poisson process during the spontaneous activity are signs of a peculiar temporal structure of the spike train. We used the ARD to characterize the bursting pattern: a hump near the origin indicates that a cell, shortly after firing a spike, is more likely to fire again. The duration of such hump corresponds to the time of cell firing deviating from a random Poisson process, hence this period might be viewed as the average burst duration (ABD). The area under the hump corresponds to the number of spikes exceeding the one expected for a random Poisson process. Therefore, from the area of the hump it is possible to compute the average number of spikes in the burst, called average burst size (ABS) (Villa 1990). The ABS to ABD ratio gives an estimation of the average intra-burst frequency (ABF). In order to avoid bias dependent on the type of distribution, comparisons between distributions of samples having different sizes were performed using the bootstrap test, based on a large number of iterations of computer-generated sampling (Diaconis and Bradley 1983).

The functional properties determined on the renewal histograms and on the dot displays, as well as the standard coordinates corresponding to the recording sites of the single units, were entered in a computerized relational database.

Acoustical stimulation

The animals were placed in a sound attenuating room. The stimuli consisted of pure tones and white noise bursts, 200 ms in duration

with a rise and fall time of 10 ms. Stimuli were delivered at a rate of 1 per second through 1/2-inch earphones (Bruel and Kjaer, type 4134). Stimulus intensities ranged approximately between 20 and 40 dB above threshold, i.e. close to 60 dB SPL for the majority of units.

The best frequency (BF) and the width of response ranges were determined by presenting tone bursts, whose frequency was linearly increased from 0.2 to 50 kHz at each stimulus. The bandwidth (BW) for one type of response pattern corresponded to the difference, in octaves, between the highest frequency and the lowest frequency evoking that pattern. These frequency ranges were rarely measured at more than one intensity and the BF was estimated by visual inspection of the dot display. It corresponded to the acoustical frequency evoking the strongest excitatory response at the shortest latency.

Results

The total number of units recorded in the present analysis was 355, along 45 electrode penetrations in 9 cats (Table 1). The majority of these units ($n=288$) were well isolated during the whole experimental protocol and recovered their activity after the cooling of AI, when compared to the control condition. The remaining units, which either did not recover completely after the cortical inactivation or were lost before the end of the protocol, were not considered further in the analyses.

The criterion for accepting a single unit return to control was the absence of a statistical difference (chi-square, $P < 0.05$) for three out of four major characteristic parameters of the firing activity (i.e., the spontaneous firing rate, ABD, ABS, and the ratio of the PST peak to the spontaneous firing rate). To determine whether a change occurred during cooling, we compared the combined pre- and post-cooling values to the during-cooling value. The deviation was considered significant when it was larger than three times the standard deviation which means a confidence limit of 99%.

Therefore, the first step in the unit classification consisted in defining the effect of cooling on that unit—i.e. increasing, unchanging, or decreasing a given parameter of firing. Based on this classification the units were grouped within an anatomical subdivision. Thus, all units increasing a given parameter (e.g. the spontaneous firing rate) formed one group. All units unaffected by the cortical

Table 1. Sampling of the anatomical subdivisions of the auditory thalamus

Anatomical subdivision	Electrode penetrations	Recorded units	Analyzed units
UND	11	72	53
BIN	4	31	24
D	5	32	29
SG	4	34	25
LV	5	55	48
M	4	52	43
OV	3	11	9
POL	3	18	15
RE	5	46	39
SCd	1	4	3
Total	45*	355	288

* Number of different tracks

Table 2. Spontaneous firing rate at normal temperature pre-cooling (n) (spikes/s \pm s.e.m.) and at post-cooling condition (p); all units are here classified according to the effect of cooling on that rate

Anatomical subdivision		Effect of cooling		
		Increased firing	Unchanged firing	Decreased firing
D	n	7.2 \pm 0.3	5.4 \pm 1.6	4.9 \pm 0.8
	p	8.2 \pm 3.0	4.7 \pm 1.3	4.7 \pm 0.9
	($N=29$)	($n=2$)	($n=9$)	($n=18$)
SG	n	9.7 \pm 3.5	7.9 \pm 2.2	11.9 \pm 2.2
	p	13.8 \pm 3.5	9.2 \pm 3.2	9.3 \pm 1.8
	($N=25$)	($n=5$)	($n=7$)	($n=13$)
LV	n	3.1 \pm 0.8	5.4 \pm 1.4	8.1 \pm 0.8
	p	3.2 \pm 1.1	6.1 \pm 1.2	7.6 \pm 2.1
	($N=48$)	($n=5$)	($n=12$)	($n=31$)
M	n	8.8 \pm 2.3	5.6 \pm 1.2	9.5 \pm 1.7
	p	6.2 \pm 1.5	6.2 \pm 0.8	7.0 \pm 1.2
	($N=43$)	($n=11$)	($n=10$)	($n=22$)
RE	n	16.8 \pm 6.5	8.9 \pm 2.4	17.3 \pm 2.6
	p	11.1 \pm 5.5	10.9 \pm 2.6	13.5 \pm 2.1
	($N=39$)	($n=7$)	($n=7$)	($n=25$)

cooling with respect to that parameter formed another group and all units decreasing that parameter formed a third group. An example of pre- and post-cooling grouped data is shown at Table 2.

Of the population of 288 analyzed units, 53 could not be unequivocally attributed to an auditory thalamic subdivision and formed the undefined (UND) subdivision; 3 cells belonged to the deeper laminae of the superior colliculus (SCd).

Spontaneous activity

In the absence of a controlled acoustical stimulation, the activity of the single units in the auditory thalamus is referred to as spontaneous. All units were spontaneously active. The spontaneous firing rate tended to decrease on average in all anatomical subdivisions of the auditory thalamus when AI was inactivated. Nevertheless 20% of the units were not modified and 20% increased their firing rate.

The relative proportions of units increasing, maintaining, or decreasing their spontaneous activity varied among the anatomical subdivisions. The group of units increasing the spontaneous firing rate in LV showed an average value of 3.1 spikes/s during the physiological condition; the average firing rate of the group decreasing the spontaneous activity was 8.1 spikes/s (Table 3). This difference was statistically significant (t -test, $P < 0.001$) and distinguished LV from the other subdivisions of the MGB. Indeed, in D, M, SG, and RE no significant difference was observed at the physiological condition in the average discharge rates of the groups of cells increasing or decreasing firing during cortical cooling (Fig. 4a).

Most units (255/288) had a tendency to fire in a non-regular Poisson process showing significant deviations in the shape of the autorenewal density histogram (ARD).

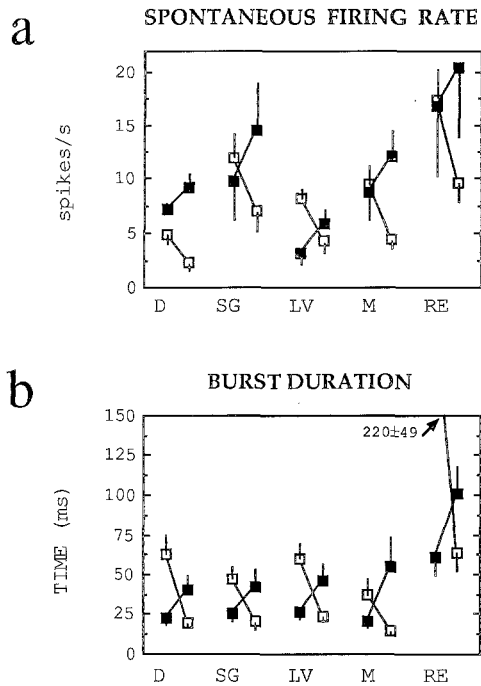


Fig. 4. **a** Plot of the average (\pm s.e.m.) spontaneous firing rate before and during cooling of the ipsilateral auditory cortex in five subdivisions of the auditory thalamus. The black squares indicate the group of units increasing the functional property, namely the firing rate in this case, during cooling and the white squares the group decreasing. Note the distinct pattern of LV compared to the other subdivisions. **b** Plot of the average (\pm s.e.m.) burst duration

The data concerning the averaged burst duration (ABD), the averaged burst size (ABS), and the averaged intra-burst frequency (ABF) were analyzed separately. Only 57 units did not show any statistically significant variation of these bursting parameters.

The cortical inactivation decreased the ABD in 103/255 units, particularly in LV, OV and D, where the proportion represented more than half of the units. In contrast only 30% of the units showed a decrease of ABD in SG, POL and RE. The difference between these two groups of subdivisions was significant (bootstrap test, $P < 0.01$). The pattern of distribution of the ABD in the groups of cells increasing or decreasing this parameter during the cryogenic blockade of AI is shown in Fig. 4b. The subdivisions LV, OV and POL were characterized by a larger proportion of units decreasing (45%) than increasing (20%) the ABS, whereas the effect tended to be opposite in SG (bootstrap test, $P < 0.01$). In all subdivisions, half of the units (148/255) maintained unchanged the ABF during the inactivation of AI. This group was formed by those units whose bursting parameters were not affected as well as by those units whose ABD and ABS were affected in the same direction and in a similar extent by the cryogenic blockade.

No significant correlation between the corticofugal effect on the bursting pattern and the firing rate could be found. Units which never fired in bursts under physiological conditions were extremely rare ($n = 6$), and their

spontaneous activity always tended to decrease during the cortical inactivation. The same corticofugal modulation was observed for the units characterized by the appearance ($n = 6$) (Fig. 5) or the disappearance ($n = 2$) of the bursting pattern during the cooling of AI.

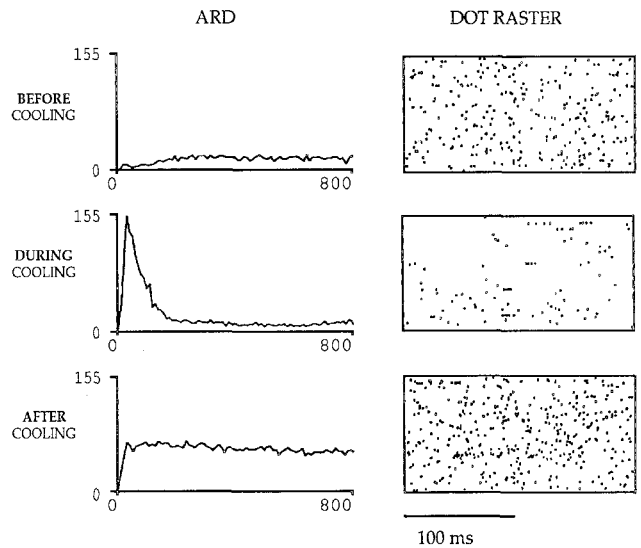


Fig. 5. Autorenewal density (ARD) and raster display of a single unit during spontaneous activity. This unit belongs to LV-BIN. Note the appearance of bursts of spikes (corresponding to the hump in the ARD) and the decrease of activity during cooling of the auditory cortex. However, after cooling this unit recovered to a discharge rate that was higher than before cooling. In the ARD the abscissa full scale is 800 ms and the ordinate full scale is 155 spikes/s. In the raster display the bar length correspond to 100 ms and 50 rasters are shown

Responses to pure tones

Out of 288 units, 214 were tested with pure tones. Only 12 units never responded to tonal stimulation no matter what the state of activation of the auditory cortex was. If a unit

Table 3. Bandwidths (octaves \pm s.e.m.) of suppressive responses to tonal stimulation at normal temperature (n) and during cortical cooling (c). All units are here classified according to the effect of cooling on the bandwidth and grouped by anatomical subdivision. The significance of disparity is computed by analysis of variance

Anatomical subdivision		Effect of cooling		significance of disparity
		Increased bandwidth	Decreased bandwidth	
D	n	4.3 ± 1.0	4.7 ± 0.8	n.s.
	c	6.7 ± 0.5	1.3 ± 0.5	< 0.001
SG	n	2.9 ± 0.4	5.6 ± 0.5	0.002
	c	4.4 ± 0.4	2.9 ± 0.8	0.091
LV	n	3.5 ± 1.5	6.0 ± 0.4	n.s.
	c	6.5 ± 0.7	3.1 ± 0.5	0.005
M	n	2.4 ± 0.7	6.4 ± 0.6	< 0.001
	c	4.8 ± 1.0	1.9 ± 0.7	0.026
RE	n	3.5 ± 0.8	4.8 ± 0.7	n.s.
	c	6.5 ± 0.5	1.0 ± 0.5	< 0.001

had a complex temporal pattern of response, its components were considered separately. Such complex response patterns were often dependent on the tone frequency and the cortical state; therefore the width of response ranges (BW) was determined for each component of the response pattern.

Excitatory early-onset transient responses, with a latency shorter than 30 ms, were observed in the majority

(76%) of the units (e.g. Fig. 6b, d, e, before cooling). Only 1/5 of these units were characterized by BWs which remained unchanged during the cortical inactivation. Late-onset as well as offset evoked responses to pure tones, observed in less than half of the units, differed by their tendency to completely disappear or appear during the inactivation of AI (e.g. Fig. 6a-offset response-, c). The cortical cooling usually induced an increase of the width of

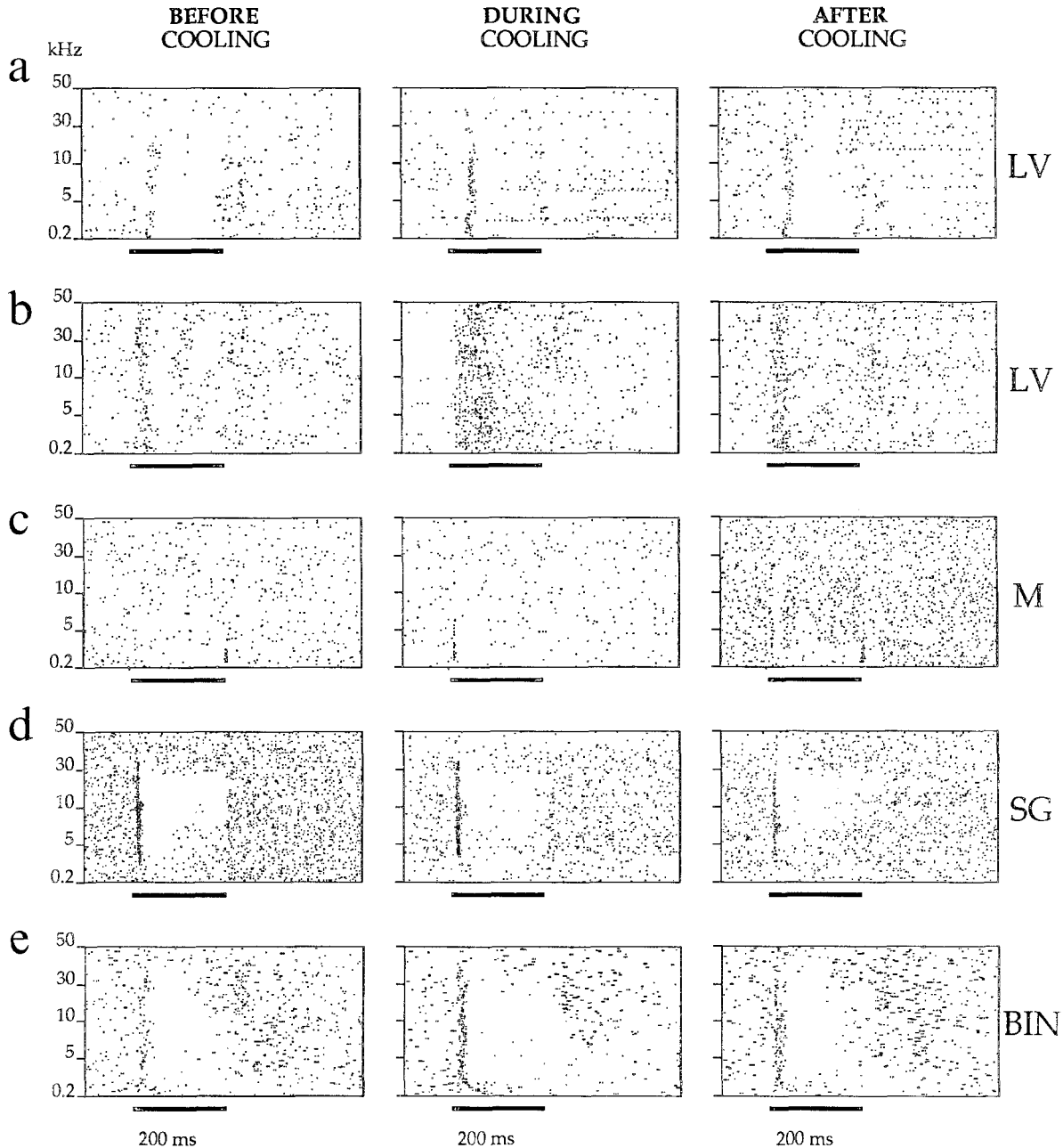


Fig. 6a–e. Raster display of single units during pure tones stimulation. Each stimulus lasted 200 ms (horizontal bar) and the frequency was linearly increased from 0.2 to 10.2 and from 10 to 50 kHz by 200 steps. **a** Unit in LV. Note the decrease of the sustained inhibition and offset response, and the increase of onset transient excitation during cortical cooling. **b** Unit in LV. Note the prolonged onset excitation

and decrease of spontaneous activity. **c** Unit in M. Note the disappearance of the offset and the appearance of an onset transient excitatory response during cooling. **d** Unit in SG. Note the stability of the response range. **e** Unit in BIN. Note an increase of onset transient excitation and sustained inhibition. During cooling note that there is also an offset inhibition over a wide range of frequencies

excitatory response ranges for long latency responses, whereas it had the opposite effect on short latency responses.

Within any given anatomical subdivision and for a given response pattern, the units were classified according to the tendency of their BW to increase or to decrease during inactivation of AI. A good disparity was characterized by a large difference between the average BW (in octaves) of these two groups (analysis of variance, $P < 0.1$). Table III exemplifies this analysis for the suppressive onset responses. Good disparity was observed before the inactivation of AI in M for the early-onset BW and in LV, RE and SG for the excitatory offset BW. D differed from the other subdivisions in having a good disparity for the suppressive (Fig. 7) and long latency excitatory responses during the cortical inactivation.

The best frequency (BF) could be determined in 175 units (Fig. 8). In most cases (124/175) the BF could be determined during both physiological conditions and during cooling of AI. In this sample the difference between the BFs in the two recording conditions was larger than 0.5 octave in 34 units (Fig. 8). Furthermore, the cortical inactivation led to a disappearance of the BF in 30 units and the appearance of a BF in 21 units.

Responses to white noise

The responses to white noise bursts were analyzed on the basis of the shape of the peristimulus time histograms (PST) of 221 units out of 228. The vast majority of units recovered the same pattern of response after the cortical inactivation, even in fine details (Fig. 9). However, a significant number of units ($n = 54$, 19%) did not recover exactly the same pattern of response to white noise although the spontaneous activity pattern did (i.e., spontaneous firing rate, ABD, and ABS). These units were more abundant in BIN, D, and OV, forming an overall proportion of almost 35%.

One of the parameters chosen to describe the responsiveness to white noise bursts is the highest peak of the PST. This value was modulated by the auditory cortex for the majority of the units (80%). The ratio between this peak of firing rate and the spontaneous firing rate can be considered as an analogue of the signal-to-noise ratio. In

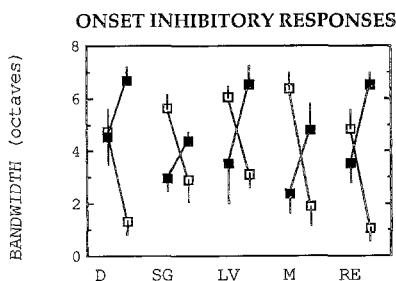


Fig. 7. Plot of the average (\pm s.e.m.) bandwidth of the onset inhibitory responses to pure tone stimulation. The same conventions of Fig. 4 are applied. Note the distinct pattern of D and RE compared to the other subdivisions

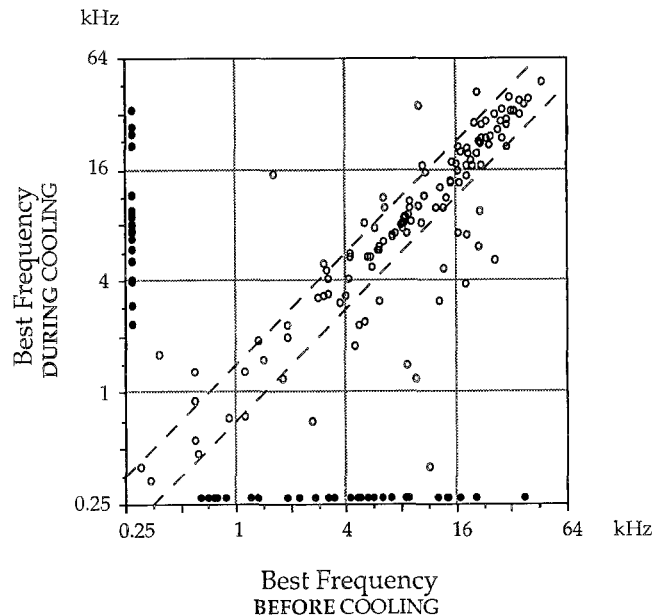


Fig. 8. Scattergram of the best frequency (BF) of tuning before vs. during cortical cooling. The white circles represent those units whose BF could be determined in all recording conditions. The dashed lines indicate a range of confidence ± 0.5 octaves. The black circles on the abscissa represent units whose BF disappeared with cortical cooling. The black circles on the ordinate represent the BF during cooling of units without clear response to pure tones at the physiological condition

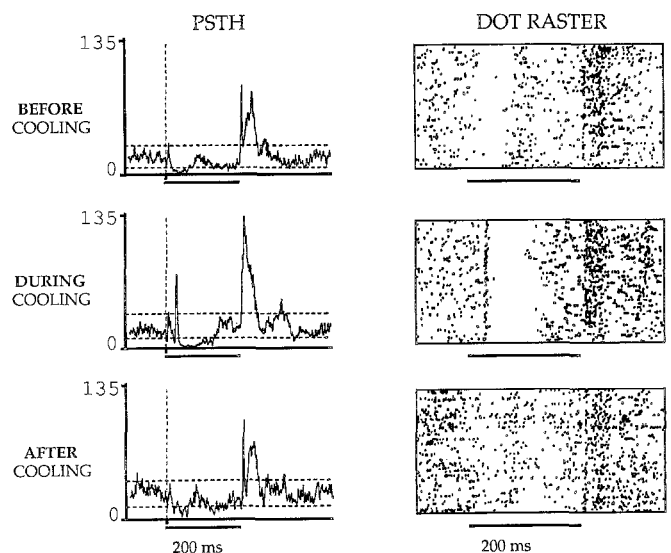


Fig. 9. Peristimulus time histogram (PST) and raster display of a single unit during acoustically evoked activity by white noise bursts lasting 200 ms (horizontal bar). This unit belongs to SG. Note the appearance of an onset transient excitatory response followed by a strong inhibition and a change of the offset transient response provoked by cooling the ipsilateral auditory cortex. In the PSTH the abscissa full scale is 550 ms and the ordinate full scale is 135 spikes/s. Dashed lines correspond to 99% confidence levels. In the raster display the horizontal bar corresponds to the stimulus delivery time and 100 repetitions are shown

half of the units the corticofugal modulation provoked a variation of the PST peak in the same direction than the spontaneous firing rate, especially in POL, RE, D, and OV. In the other regions (Fig. 9), LV and BIN particularly, the effect of the cortical inactivation selectively affected the signal-to-noise ratio, almost always in the sense of increasing it during the cooling of AI. The distinction of these groups of subdivisions was statistically significant (bootstrap test, $P < 0.05$).

The onset transients with a latency shorter than 30 ms were much less affected by the cortical cooling, when compared to the responses to pure tones. The examination of the temporal response pattern indicated that the corticofugal modulation more often affected the responses at longer latencies from the stimulus onset (e.g., appearance of a late-onset transient excitation followed by a sharp suppression, Fig. 9). In LV and POL almost no units remained unaffected after the white noise burst offset.

Discussion

Contradictory data have been reported regarding the effect of the corticofugal influence on the activity of the auditory thalamus (Amato et al. 1969; Aitkin and Dunlop 1969; Ryugo and Weinberger 1976; Orman and Humphrey 1981). Our efforts to elucidate the functional role of the pathways involved were directed towards the examination of a large number of the functional properties of the thalamic cells before and during the inactivation of the primary auditory cortex. The present study has resolved some of the contradictory data reported in the literature: (i) no thalamic unit remained unaffected by cortical cooling when all functional properties were considered; (ii) the primary auditory cortex exerts a mainly excitatory influence on the auditory thalamus; (iii) consistent differences of the corticofugal effect have been observed among the thalamic subdivisions; (iv) cortically controlled activity in cell assemblies of the auditory thalamus might set up the adaptive filtering of the ascending sensory input.

The first conclusion which can be drawn from our findings is that all units which recovered their characteristics after the cortical cooling were affected in some way by the cortical modulation, for at least one of the functional properties analyzed here. This proportion is larger than that reported in previous studies, but can probably be explained by the large number of functional properties examined in the present investigation. A similar observation in the visual pathway has already been reported (Geisert et al. 1981).

Some methodological side effects could have contributed to alter the neuronal activity in the thalamus. One is the unspecific effect of the cortical cooling on the cerebral blood flow or on the MGB directly. No measure of the blood flow in the MGB was performed, but a change of this flow could alter unspecifically the single unit activities in the MGB. For a given cell, we observed that a change of a given functional property could occur independently of a change of the other properties and that most of the units maintained one or more properties unchanged during the cortical cooling. Therefore an alteration of the local blood

flow or a direct cooling of the MGB is not likely to account for our findings. The rectal temperature was monitored permanently and the small fluctuations of that temperature were not synchronous with the periods of cortical inactivation; thus, cooling of the systemic blood could also not account for the present findings.

The monitoring of the evoked potentials in the auditory cortex supplied evidence concerning the state of activity of the cortical area beneath the cooling device. These recordings were consistent with an inactivation of the auditory cortex during the cooling and a recovery of activity after cooling. Therefore we consider altogether that the changes of the neuronal activity in the auditory thalamus were indeed the consequence of a reversible inactivation of the auditory cortex. In most cats a portion of AI, characterized by low best frequencies (BF) is buried deeply in the posterior ectosylvian sulcus (Reale and Imig 1980) and the question of whether this portion would be inactivated could be raised. However, our results have shown that units characterized by BF lower than 8 kHz were likely to be affected more than high BF units. Thus, the cooling of the auditory cortex is assumed to inactivate all AI, and to some extent portions of surrounding cortical fields. Moreover, different corticofugal effect upon high and low BF units may suggest a different type of information processing of the sound frequencies, as suggested by auditory RE activity (Villa 1990).

In the MGB as well as in the other dorsal thalamic nuclei of the cat two major types of cells have been described on the basis of morphological criteria (Morest 1964; Guillery 1966): (1) the principal cells (P-cells), projecting to the cortex, and (2) the interneurons (I-cells), whose axons do not leave the MGB, identified as GABAergic inhibitory cells (Sterling and Davis 1980). The electric impedance of our microelectrodes was about 1 M Ω , an unfavorable value for recording the extracellular electric fields generated by the small neurons such as the I-cells (Abeles 1982b). We assume that our populations of units corresponded to P-cells.

During cortical inactivation, the majority of the units decreased the spontaneous firing rate. This finding suggests that the corticothalamic fibers exert a mainly facilitatory or excitatory role, in agreement with previous electrophysiological reports (Kalil and Chase 1970; Singer 1977; Tsumoto et al. 1978; Orman and Humphrey 1981). Some neurochemical data have been reported elsewhere suggesting that the neurotransmitter of the corticothalamic pathways may be an excitatory amino acid, thus exerting a facilitatory influence (Fonnum et al. 1981). On the basis of an heterogenous effect of cryogenic blockade of AI (e.g., 60% of the units decreased spontaneous firing rate, 20% of them increased, 20% remained unchanged), functional populations of units were identified in the auditory thalamus. We do not think that this variability reflects various neuronal populations. Rather, it could reflect the complex influence of AI activity upon the thalamus, strongly mediated by RE cells.

Because of the large number of differences which were observed among the anatomical subdivisions of the auditory thalamus, the following part of the discussion will be focused on the major characteristics of each sub-

Table 4. Corticofugal modulation on some functional properties in five subdivisions of the auditory thalamus. × reverse functional disparity (FD); ∪ disappearance of FD during cooling; ∩ appearance of FD during cooling; n.s. non-significant analysis of variance; *not enough data for statistics

Functional property	Anatomical subdivision				
	D	SG	LV	M	RE
Spontaneous activity					
Firing rate	∩	∩	∪	∩	∩
Burst duration	X	∪	X	∩	X
Burst size	∩	∩	∩	∩	X
Pure tones driven activity					
Excitatory early-ON bandwidth	X	*	n.s.	∪	n.s.
----- late-ON bandwidth	∩	*	X	X	X
----- OFF bandwidth	X	∪	∪	∩	∪
Inhibitory ON bandwidth	∩	X	∩	X	∩

division. The term of “spontaneous activity” should not be viewed as the consequence of internal thalamic pacemaker activity, but rather as the result of the activity of the neural networks within which the auditory thalamus is embedded. Thus, the characteristics of the spontaneous activity are considered as functional properties (Table 4).

Reticular nucleus of the thalamus (RE)

By considering the direct RE projection to the P-cells, it might appear surprising that the cortical inactivation of AI provoked a decrease of the spontaneous firing rate in the majority of the RE-units (65%) as well as in the dorsal auditory thalamic subdivisions. A parallel variation of the activity in the RE-cells and the P-cells was already described in other thalamic nuclei (Domich et al. 1986). One explanation could be that the RE-thalamic GABAergic projection may be excitatory, but there is evidence against this hypothesis (Roy et al. 1984). Another way to account for such finding and for an inhibitory role of the RE-thalamic projections is to consider the I-cells as a major target of this pathway (Montero and Singer 1985). In such case, a decrease of the activity in RE due to the cortical inactivation would provoke a release of the inhibition of the I-cells by the RE-cells. Consequently the I-cells would inhibit the P-cells and a decrease of the activity of RE and P-cells would appear in parallel. Similar hypotheses about a strong influence on inhibitory mechanisms and a disinhibitory role of the corticothalamic pathway were reported previously for other pathways and at a cellular level (Singer 1977; Steriade et al. 1985, 1986).

Pars lateralis of MGB and brachium of inferior colliculus (LV and BIN)

A very large proportion of units which tended to increase the signal-to-noise ratio during cortical cooling was found in LV and BIN. This finding was mostly due to a large decrease of the spontaneous activity rather than an increase of the maximum evoked firing rate. Transient onset responses to pure tones were commonly observed and the

BW tended to be modified by cortical cooling in most units. BWs are thought to depend on lateral inhibition mechanisms and the state of anesthesia (Aitkin and Webster 1972; Morel et al. 1987); therefore they are expected to change if the I-cell activity is affected, as suggested by our hypothesis. Furthermore, this finding points out to the important role played by the cortical activity upon the thalamus, even for short latency responses.

Dorsal division of MGB (D)

Looking at the effect of the cortical inactivation upon the various auditory thalamic subdivisions it is surprising that D was clearly affected, despite the fact that it is known to be poorly interconnected with AI (Andersen et al. 1980; Rouiller and de Ribaupierre 1985). This result could be due to a spread of the cooling to the adjacent areas of AI which project to D (mainly AII) or to an indirect modulation of these areas following AI inactivation via cortico-cortical connections and to the widely divergent projections of RE to the auditory thalamus (Rouiller et al. 1985). In contrast to LV, D showed a vast majority of units that decreased their maximum evoked firing rate as well as their spontaneous activity, without any significative change of the signal-to-noise ratio, thus suggesting a tonic corticofugal influence upon this subdivision.

Medial division of MGB (M)

The medial division of MGB was characterized by a moderate proportion (25%) of units which increased the spontaneous firing rate when compared to the other subdivisions (10% of the units). M is involved in multimodal sensory pathways (Wepsic 1966; Aitkin et al. 1978; Edeline 1990). Therefore, a reduced inhibitory influence by the auditory-RE-thalamic projections—due to the cooling of AI—might induce a relative increase in the efficacy of the non-auditory projections.

Suprageniculate nucleus (SG)

Another multimodal subdivision, SG (Winer, 1988; Norita and Katoh, 1987) clearly differed from other nuclei in that more than half of its units increased the maximum firing rate evoked by white noise bursts without a parallel increase of the spontaneous activity. Transient responses were commonly observed and the inhibitory responses tended to be significantly reinforced during the cryogenic blockade of the auditory cortex (Fig. 9). This could suggest that the role of SG is concerned with the transient features of the stimuli and that the inhibitory responses may introduce some “dead time” and a sequential order in the information processing.

Functional disparity

With respect to studies performed in other sensory pathways (Singer 1977; Tsumoto et al. 1978; Diamond 1983;

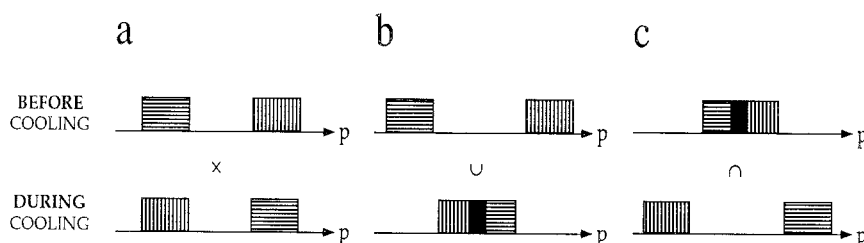


Fig. 10a-c. Theoretical model of the functional disparity (FD) for a given functional property (p). The horizontal lines and vertical lines boxes represent the group of units increasing, respectively decreasing that property during cooling. **a** FD is present before and during cooling (\times). **b** FD disappears during cooling (\cup). **c** FD appears during cooling (\cap)

Macchi et al. 1986) our findings confirm that corticofugal influences produce mostly excitatory effects in the sensory related thalamic nuclei. Therefore, further analogies might be considered in the role of cortico-thalamic feedback. Considering each functional property separately (i.e. the average burst duration or the bandwidth for a given pattern of response to pure tones) we analyzed the average value of that property for the units increasing, or decreasing, during the cortical inactivation (Table 4).

In the distribution of a given functional property, the existence of two statistically distinct means (one for the units “increasing” and one for the units “decreasing”) is interpreted as a sign of disparity. If one assumes that the group of units “decreasing” a certain functional property forms a cell assembly and those units “increasing” form another cell assembly, then such cell assemblies might be the support for coding the disparity. One hypothesis might be that clearly distinct average values correspond to two possible states of activity of the cell assemblies and that the cortical influence would “switch” between the two states (Fig. 10a). This case is called “reverse” functional disparity (FD), where the term “functional” refers to its dependence on the state of the cerebral cortex. A second case corresponds to a disappearance of disparity (Fig. 10b). The last case, in contrast to the previous one, corresponds to largely overlapping average values for groups “increasing” and “decreasing” before the cortical inactivation, then to the appearance of functional disparity during cooling (Fig. 10c). The emergence of cell assemblies, for coding the FD, has previously been reported in the coding of complex spatio-temporal patterns (Creutzfeld et al. 1980; Abeles 1982b; Villa and Abeles 1990).

We considered the FD for each subdivision separately and we observed that in 13/30 of the cases (Table 4) the FD appeared during the cortical cooling, whereas in 6 cases it disappeared. It is important to notice that the disappearance of FD involves mainly those properties defined for activity driven by pure tones. The meaning of this finding might be that the maximum efficacy of tone discrimination, as determined by the existence of bandwidth disparities, is controlled by cortical activity. We suggest that adaptive filtering could be performed by thalamic cell assemblies, which are the support of coding functional disparity. This processing would allow to selectively extract information from the incoming sensory signals according to the cortical activity. Close analogies exist between the thalamocortical neuronal circuitry and the technical description (Widrow and Stearns 1985) of adaptive filtering circuits (Fig. 11). Corticofugal activity would regulate the response properties of thalamic units by changing their bandwidth responsiveness to pure tones.

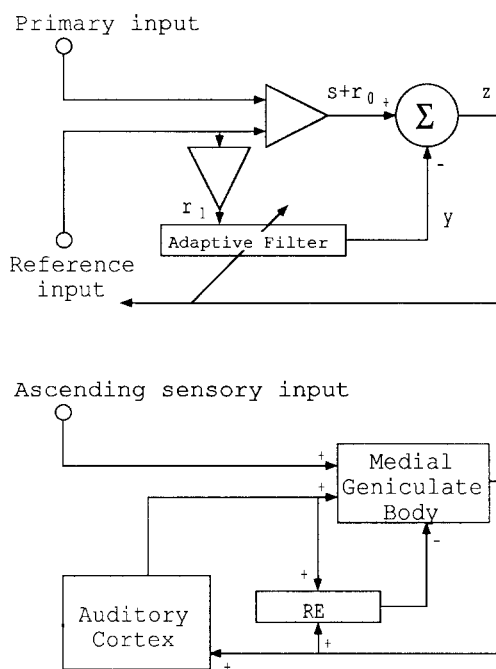


Fig. 11. Upper section: schematic drawing of adaptive signal filtering with two inputs. The primary input contains the useful signal s and a reference signal r_0 which are uncorrelated. The reference input contains a signal r_1 correlated only with r_0 . The filter's output is y and the system's output is z . For more details see Widrow and Stearns (1985). Lower section: a functional scheme of the thalamo-cortical auditory pathway, as described in the text. RE: reticular nucleus of the thalamus. Note the strong analogies between the technical circuit and the anatomical functional circuit. The corticofugal modulation of the bandwidth response to the pure tones could be due to an adaptive filtering controlled by the cortex

The observation of several functionally characterized types of units within the auditory part of RE (Villa 1990) suggest that this structure could play a key-role in “setting” the filter's coefficients.

However, the complexity of synaptic arrangements within the auditory thalamus leaves unanswered questions: how to compensate or overwhelm the simultaneous effects of RE disfacilitation onto thalamocortical neurons, local-circuit neurons and the direct influences of cortico-thalamic projections? Future studies using selective excitotoxic lesions of sectors of RE and local-circuit cells, as well as simulations of neural networks, will probably bring more precision in the understanding of corticofugal mechanisms.

Acknowledgements. This work was partly supported by grant no. 3.370.086 from the Swiss National Science Foundation. We wish to

thank Prof. M. Dolivo for his encouragement, and Prof. M. Abeles for providing some of the computer programs. We are grateful to E. Colomb, C. Eriksson, C. Rodrigues-Dagaëff, and P. Küffer for their participation in some experimental sessions, and to M. Capt, C. Haeblerli, and M. Jadé for their technical assistance. We acknowledge the critical reading of the manuscript by Drs. J.-M. Edeline, J. Fuster, and J. Quintana.

References

- Abeles M (1982a) Quantification, smoothing, and confidence limits for single unit histogram. *J Neurosci Meth* 5: 317–325
- Abeles M (1982b) Local cortical circuits: an electrophysiological study. In: *Studies of brain function*, Vol 6. Springer, Berlin New York
- Aitkin LM, Dunlop CW (1969) Inhibition in the medial geniculate body of the cat. *Exp Brain Res* 7: 68–83
- Aitkin LM, Webster WR (1972) Medial geniculate body of the cat: organization and responses to tonal stimuli of neurons in ventral division. *J Neurophysiol* 35: 365–380
- Aitkin LM, Dickhaus H, Schult W, Zimmermann M (1978) External nucleus of inferior colliculus: auditory and spinal somatosensory afferents and their interactions. *J Neurophysiol* 41: 837–847
- Amato G, LaGrutta V, Enia F (1969) The control exerted by the auditory cortex on the activity of the medial geniculate body and inferior colliculus. *Arch Sci Biol* 53: 291–313
- Andersen RA, Knight PL, Merzenich MM (1980) The thalamocortical and corticothalamic connections of AI, AII and the anterior auditory field (AAF) in the cat: evidence for two largely segregated systems of connections. *J Comp Neurol* 194: 663–701
- Brooks VB (1983) Study of brain function by local, reversible cooling. In: *Reviews of physiology, biochemistry and pharmacology*, Vol 95. Springer, Berlin, pp 1–109
- Calford MB, Aitkin LM (1983) Ascending projections to the medial geniculate body of the cat: evidence for multiple parallel auditory pathways through thalamus. *J Neurosci* 3: 2365–2380
- Creutzfeld O, Hellweg FC, Schreiner C (1980) Thalamocortical transformation of responses to complex auditory stimuli. *Exp Brain Res* 39: 87–104
- Desmedt JE, Mechelse K (1958) Suppression of acoustic input by thalamic stimulation. *Proc Soc Exp Biol (NY)* 99: 772–775
- Diamond IT (1983) Parallel pathways in the auditory, visual and somatic systems. In: *Macchi G, Rustioni A, Spreafico R (eds) Somatosensory integration in the thalamus*. Elsevier, Amsterdam, pp 251–272
- Diaconis P, Bradley E (1983) Computer-intensive methods in statistics. *Sci Am* 248: 96–108
- Domich L, Oakson G, Steriade M (1986) Thalamic burst patterns in naturally sleeping cat: a comparison between cortically projecting and reticularis neurons. *J Physiol (London)* 379: 429–449
- Fonnum F, Storm-Mathisen J, Divac I (1981) Biochemical evidence for glutamate as neurotransmitter in corticostriatal and corticothalamic fibres in rat brain. *Neuroscience* 6: 863–873
- Edeline J-M (1990) Frequency specific plasticity of single unit discharge in the rat medial geniculate body. *Brain Res* 529: 109–119
- Geisert EE, Langsetmo A, Spear PD (1981) Influence of the cortico-geniculate pathway on response properties of cat lateral geniculate neurons. *Brain Res* 208: 409–415
- Guillery RW (1966) A study of Golgi preparations from the dorsal lateral geniculate nucleus of the adult cat. *J Comp Neurol* 128: 21–50
- Heath CJ, Jones EG (1971) An experimental study of ascending connections of the posterior group of thalamic nuclei in the cat. *J Comp Neurol* 141: 397–426
- Ivarsson C, de Ribaupierre Y, de Ribaupierre F (1988) Influence of auditory localization cues on neuronal activity in the auditory thalamus of the cat. *J Neurophysiol* 59: 586–606
- Jones EG (1975) Some aspects of the organization of the thalamic reticular complex. *J Comp Neurol* 162: 285–308
- Kalil RE, Chase R (1970) Corticofugal influence on activity of lateral geniculate neurons in the cat. *J Neurophysiol* 33: 459–474
- Macchi G, Bentivoglio M, Minciaccchi D, Molinari M (1986) Organisation des connexions thalamiques. *Rev Neurol (Paris)* 142: 267–282
- Mitani A, Itoh K, Mizuno N (1987) Distribution and size of thalamic neurons projecting to layer I of the auditory cortical fields of the cat compared to those projecting to layer IV. *J Comp Neurol* 257: 105–121
- Montero VM, Singer W (1985) Ultrastructural identification of somata and neural processes immunoreactive to antibodies against glutamic acid decarboxylase (GAD) in the dorsal lateral geniculate nucleus of the cat. *Exp Brain Res* 59: 151–165
- Morel A, Rouiller E, de Ribaupierre Y, de Ribaupierre F (1987) Tonotopic organization in the medial geniculate body (MGB) of lightly anesthetized cats. *Exp Brain Res* 69: 24–42
- Morel A, Imig TJ (1987) Thalamic projections to fields A, AI, P, VP in cat auditory cortex. *J Comp Neurol* 265: 119–144
- Morest DK (1964) The neuronal architecture of the medial geniculate body of the cat. *J Anat* 98: 611–630
- Norita M, Katoh Y (1987) The GABAergic neurons and axon terminals in the lateralis medialis-suprageniculate nuclear complex of the cat: GABA-immunocytochemical and WGA-HRP studies by light and electron microscopy. *J Comp Neurol* 263: 54–67
- Orman SS, Humphrey GL (1981) Effects of changes in cortical arousal and of auditory cortex cooling on neuronal activity in the medial geniculate body. *Exp Brain Res* 42: 475–482
- Purser BD, Whitfield IC (1972) Thalamo-cortical connections and tonotopicity in the cat medial geniculate body. *J Physiol* 222: 161–162
- Reale RA, Imig TJ (1980) Tonotopic organization of auditory cortex in the cat. *J Comp Neurol* 192: 265–291
- Rodrigues-Dagaëff C, Simm G, de Ribaupierre Y, Villa A, de Ribaupierre F, Rouiller EM (1989) Functional organization of the ventral division of the medial geniculate body of the cat. Evidence for a rostro-caudal gradient of response properties and cortical projections. *Hear Res* 39: 103–126
- Rose JE, Galambos R (1952) Microelectrode studies on medial geniculate body of cat. I. Thalamic region activated by click stimuli. *J Neurophysiol* 15: 343–357
- Rouiller EM, Colomb E, Capt M, de Ribaupierre F (1985) Projections of the reticular complex of the thalamus onto physiologically characterized regions of the medial geniculate body. *Neurosci Lett* 53: 227–232
- Rouiller EM, Rodrigues-Dagaëff C, Simm G, de Ribaupierre Y, Villa A, de Ribaupierre F (1989) Functional organization of the medial division of the medial geniculate body of the cat: tonotopic organization, spatial distribution of response properties and cortical connections. *Hear Res* 39: 127–142
- Rouiller EM, de Ribaupierre F (1985) Origin of afferents to physiologically defined regions of the medial geniculate body of the cat: ventral and dorsal divisions. *Hear Res* 19: 97–114
- Roy JP, Clercq M, Steriade M, Deschênes M (1984) Electrophysiology of neurons of the lateral thalamic nuclei in cat: mechanisms of long-lasting hyperpolarizations. *J Neurophysiol* 51: 1220–1235
- Ryugo DK, Weinberger NM (1976) Corticofugal modulation of the medial geniculate body. *Exp Neurol* 51: 377–391
- Singer W (1977) Control of thalamic transmission by corticofugal and ascending reticular pathways in the visual system. *Physiol Rev* 57: 386–420
- Sterling P, Davis TL (1980) Neurons in cat lateral geniculate nucleus that concentrate exogenous ³H-g-aminobutyric acid (GABA). *J Comp Neurol* 192: 737–749
- Steriade M, Deschênes M, Domich L, Mulle C (1985) Abolition of spindle oscillations in thalamic neurons disconnected from nucleus reticularis thalami. *J Neurophysiol* 54: 1473–1497
- Steriade M, Domich L, Oakson G (1986) Reticularis thalami neurons revisited: activity changes during shifts in states of vigilance. *J Neurosci* 6: 68–81

- Tsumoto T, Creutzfeldt OD, Legédy CR (1978) Functional organization of the corticofugal system from visual cortex to lateral geniculate nucleus in the cat (with an appendix on geniculocortical mono-synaptic connections). *Exp Brain Res* 32: 345–364
- Villa AEP, Colomb E, Ericksson C, Küffer P, de Ribaupierre Y, de Ribaupierre F (1984) Corticofugal influence on single unit activity in the Medial Geniculate Body (MGB) assessed by cortical cooling. *Experientia* 40: 600
- Villa AEP (1988) Influence de l'écorce cérébrale sur l'activité spontanée et évoquée du thalamus auditif du chat. Ph.D. Thesis, University of Lausanne, Lausanne, Switzerland
- Villa AEP, Rouiller EM, Simm GM, Zurita P, de Ribaupierre Y, de Ribaupierre F (1989) Corticofugal modulation of the functional selectivity in the auditory thalamus of the cat. *Eur J Neurosci Suppl* 2: 324
- Villa AEP (1990) Functional differentiation within the auditory part of the thalamic reticular nucleus of the cat. *Brain Res Rev* 15: 25–40
- Villa AEP, Abeles M (1990) Evidence for spatio-temporal firing patterns within the auditory thalamus of the cat. *Brain Res* 509: 325–327
- Watanabe T, Yanagiswara K, Kanzaki J, Katsuki Y (1966) Cortical efferent flow influencing unit responses of medial geniculate body to sound stimulation. *Exp Brain Res* 2: 302–317
- Wepsic JG (1966) Multimodal sensory activation of cells in the magnocellular medial geniculate nucleus. *Exp Neurol* 15: 299–318
- Widrow B, Stearns S (1985) Adaptive signal processing. Prentice Hall, Englewood Cliffs
- Winer JA, Diamond IT, Raczkowski D (1977) Subdivisions of the auditory cortex of the cat: the retrograde transport of horseradish peroxidase to the medial geniculate body and posterior thalamic nuclei. *J Comp Neurol* 176: 387–418
- Winer JA (1988) Anatomy of the medial geniculate body. In: Altschuler RA, Hoffman DW, Bobbin RP, Clopton BM (eds) *Neurobiology of hearing, Vol 2. The central auditory system*. Raven Press, New York
- Yuan B, Morrow TJ, Casey KL (1986) Corticofugal influences of S1 cortex on ventrobasal thalamic neurons in the awake rat. *J Neurosci* 6: 3611–3617
- Zurita P, Villa AEP, Simm GM, Rouiller EM, de Ribaupierre Y, de Ribaupierre F (1988) Effects of pentobarbital and ketamine on thalamic and cortical auditory neurons of the cat. *Eur J Neurosci Suppl* 1: 164